DEVELOPMENT OF AN EARTHQUAKE ISOLATION DEVICE USING RUBBER BEARING AND FRICTION DAMPER

by

Takafumi FUJITA,[I] Satoshi FUJITA,[II] and Toshikazu YOSHIZAWA[III]

SYNOPSIS

This paper deals with a new type of earthquake isolation device for mounting between a foundation and a base of heavy mechanical and/or electrical equipment to efficiently protect the superstructure from an earthquake attack. The device consists of a laminated rubber bearing which is designed to be very soft horizontally and very stiff vertically (the ratio of vertical stiffness to horizontal one of the bearing is about 1600), a friction damper which introduces energy-absorbing capability into the system and a back-up structure which prevents the superstructure from landing by the P-Δ effect.

Static and dynamic tests on the full-sized devices of which the vertical load capacity was 98kN were carried out and various fundamental properties of the device, the rubber bearing and the friction damper were checked. Then it was concluded the device possessed the performance required for the earthquake isolation of heavy equipment.

INTRODUCTION

The isolation device adopted for the isolation of earthquake vibration in heavy mechanical or electrical equipments must be designed to withstand the large scale of vertical load and possess the very low horizontal natural frequency required to give adequate earthquake protection. The laminated rubber bearing in Fig. 1 , comprising natural rubber sheets and metal plates stacked one upon another alternately and connected together, satisfies the above-mentioned requirements and has been used as bridge bearing in Europe for long years.[1)]

In this study, a new type of earthquake isolation device using the laminated rubber bearing and the friction damper is proposed. Up to the present, the experimental tests of an actual-sized isolation device (load capacity is 98kN=10000kgf) were carried out using actuators equiped in the Chiba Experiment Station, the Institute of Industrial Science, University of Tokyo.

ISOLATION DEVICE

Installing the laminated rubber bearing in between a superstructure and a foundation, horizontal natural frequency of the total system is much lower and earthquake response acceleration of the superstructure is reduced remarkably. But, on the other hand, the response displacement is generally

---

I) Professor Associate, Institute of Industrial Science, University of Tokyo.
II) Research Associate, Institute of Industrial Science, University of Tokyo.
III) Engineer, Bridgestone Tire Co., Ltd., Development Dept

increased. In addition, at worst, the laminated rubber bearing itself can be subjected to damage. In order to overcome the above-mensioned difficulty, another device so called the friction damper is also installed in the device. The friction damper set on the annular member of the device introduces energy-absorbing capability into the system to reduce resonance effects and keep deflexion within an acceptable limit.

Fundamental concept of the isolation device is schematically shown in Fig. 2. The laminated rubber bearing, installed at the center of the device, is fixed to both a lower surface of the superstructure and a foundation and bears most of the weight of the superstructure. The friction damper, comprising an annular member of an inverted U-shaped section and several friction plates set on this member, is mounted on an annular guide wall and gives the superstructure a proper friction damping adjusted by the coil springs. Also, the annular guide wall is a kind of a back-up structure which prevents the superstructure from landing by the P-Δ effect.

PRE-ANALYSIS OF ISOLATION EFFECTS

A superstructure supported on an isolation device which allows horizontal base motion is approximated by the mathematical model of a single degree of freedom as shown in Fig. 3. We can obtain the equation of motion as follows.

(i) Friction damper is in steady contact with superstructure --Phase I

$$m\ddot{x}_G + c\dot{x}_G + k(x_G - x_B) = -m\ddot{z}_H \tag{1}$$

$$x_B = \text{const.} \quad , \quad \dot{x}_B = 0 \tag{2}$$

(ii) Friction damper is in sliding contact with superstructure--Phase II

$$m\ddot{x}_G + c(\dot{x}_G - \dot{x}_B) + k(x_G - x_B) = -m\ddot{z}_H \tag{3}$$

$$c(\dot{x}_G - \dot{x}_B) + k(x_G - x_B) = C_H\dot{x}_B + F_K \cdot \mathrm{sgn}(\dot{x}_B) + K_H x_B \tag{4}$$

(iii) Conditions of Phase switchover

$$\text{If} \quad |c\dot{x}_G + k(x_G - x_B) - K_H x_B| > F_S \ , \qquad \text{Phase I} \rightarrow \text{Phase II} \tag{5}$$

$$\text{If} \quad \dot{x}_B = 0 \ \text{and} \ |c\dot{x}_G + k(x_G - x_B) - K_H x_B| \leq F_S \ , \qquad \text{Phase II} \rightarrow \text{Phase I} \tag{6}$$

where x_G and x_B are relative displacements of the center of gravity and the base of superstructure respectively to the ground, m, c, k mass, damping constant and spring constant of superstructure respectively, K_H, C_H total horizontal spring constant and damping constant of laminated rubber bearing respectively, F_K, F_S kinematic and static friction force respectively and $\ddot{z}_H$ is horizontal acceleration of ground motion. Moreover, the following relationships are introduced.

$$\omega_0 = \sqrt{k/m} \ , \quad 2\eta = c/\sqrt{mk} \ , \quad \Omega_H = \sqrt{K_H/m} \ , \quad 2\zeta_H = C_H/\sqrt{mK_H} \tag{7}$$

$$\bar{\mu}_S = F_S/(mg) \ , \quad \bar{\mu}_K = F_K/(mg)$$

Fig. 4 shows the effects of T_H and $\bar{\mu}_K$ on the response acceleration and displacement of superstructure to three ground motions ; El Centro NS 300 Gal, Hachinohe NS 300 Gal and Tohoku Univ. NS 300 Gal (ω_0=31.4 rad/sec, $\eta = \zeta_H = 0.03$). It is given that the device provides effective earthquake

isolation when the horizontal natural period of isolated equipment is 2.0sec and the apparent coefficient of friction is 0.08. Fig. 5 shows the time histories of responses to Hachinohe NS 300Gal. Fig. 6 gives the maximum response accelerations of both isolated and non-isolated superstructure for periods of superstructure up to 1.0sec.

DESIGN OF THE LAMINATED RUBBER BEARING

VERTICAL SPRING CONSTANT: The relationship between the apparent compression modulus E_{ap} and the Young's modulus E_0 is given as follows,

$$E_{ap} = E_0(1 + 2\kappa S^2) \tag{8}$$

where, κ is a numerical factor and S is a shape factor. For a circular sheet, a shape factor is

$$S = A_R / (\pi d_R t_R) = d_R / (4t_R) \tag{9}$$

where, t_R is a thickness of a layer of rubber sheets, d_R a diameter and $A_R(=\pi d_R^2/4)$ is a loaded area. Therefore, the vertical spring constant K_{V0} of n-layer unit is given as follows,

$$K_{V0} = A_R E_{ap} / (nt_R) \tag{10}$$

HORIZONTAL SPRING CONSTANT: Considering the shear and bending deformation, the horizontal spring constant K_{H0} of n-layer unit may be obtained as

$$\{ nt_R/(A_R G) + n^3 t_R^3/(12E_0 I) \}^{-1} < K_{H0} < \{ nt_R/(A_R G) + n^3 t_R^3/(12E_{ap} I) \}^{-1} \tag{11}$$

where, G is the shear modulus and $I(=\pi d_R^4/64)$ is the moment of inertia.

CONDITIONS OF DESIGN: The laminated rubber bearing, for the loaded mass m_0 and the maximum allowable deflexion Δ_a, must be designed to fulfill the following conditions,

$$f_{V0} = \sqrt{K_{V0} / m_0} / (2\pi) \geq 15\text{Hz} \tag{12}$$

$$f_{H0} = \sqrt{K_{H0} / m_0} / (2\pi) = 0.5\text{Hz} \tag{13}$$

$$\varepsilon_t = \Delta_a / (nt_R) + 6Sm_0 g / (E_{ap} A_D) \leq \varepsilon_B / 2 \tag{14}$$

where,

$$A_D = \{ d_R^2 \sin^{-1}(\sqrt{d_R^2 - \Delta_a^2} / d_R) - \Delta_a \sqrt{d_R^2 - \Delta_a^2} \} / 2$$

where, A_D is the loaded area at the maximum allowable deflexion and ε_B is the elongnation at break. Eqs. (14) shows that the total equivalent shear strain, which is the sum of the strain due to shear and the maximum shear strain due to loads normal to the bearing surface, must be equal to or less than a harf of the elongnation at break.[2)]

The laminated rubber bearing, manufactured by trial for m_0 = 10000kg and Δ_a = 12cm, possesses the following specifications.

G = 0.50MPa(5.1kgf/cm^2) , E_0 = 0.98MPa(10.0kgf/cm^2) ,

Hardness(IRHD) = 40 , t_R = 0.25cm , d_R = 19.5cm , n =53 ,

K_{V0} = 1.4 × 10^{5}kN/m(1.5 × 10^{5}kgf/cm) , f_{V0} = 19Hz > 15Hz ,

$86kN/m(\ 87kgf/cm\ ) < K_{H0} < 113kN/m(\ 115kgf/cm\ )\ ,\ 0.47Hz < f_{H0} < 0.53Hz\ ,$

$\varepsilon_t = 3.2 < 3.6 = \varepsilon_B / 2$

EXPERIMENTAL MODEL AND TESTING FACILITY

Four laminated rubber bearings as shown in Fig. 7 and two isolation devices as shown in Fig. 8 and Fig. 9 were manufactured by trial. The experimental tests were carried out using the actuators, which applies the horizontal displacements and the vertical forces instead of the loads to be caused by the superstructure, as shown in Fig. 10.

TEST PROGRAMME

Several transducers and sensors were installed as shown in Fig. 10. Displacements and reaction forces at various points were measured, including reaction forces at both of the actuators, horizontal relative displacements between the isolation devices and the sliding plate, vertical relative displacements between the isolation devices and the rigid frame of test set-up and vertical reaction forces at the friction dampers using strain gauges set on coil springs on the isolation devices.

Four laminated rubber bearings were devided into two pairs of R.B.1.2 and R.B.3.4. First, Friction Damper Test I was carried out to measure the coefficients of static and kinematic friction mainly, secondly Rubber Bearing Test I using R.B.1.2, including the creep test of 100 hours, was carried and thirdly Isolation Device Test I was carried out. Moreover, Friction Damper Test II, Rubber Bearing Test II using R.B.3.4 and Isolation Device Test II were carried out.

RESULTS OF THE EXPERIMENTAL TESTS

FRICTION DAMPER TEST: In Fig. 11(a),(b),(c), examples of characteristics of friction forces are shown. (a) shows the initial variations of friction force, and after about ten cycles, the friction force is gradually reduced to the steady level as shown in (b). The increase of vertical load gives the proper level of friction force 7.84kN(800kgf) as shown in (c). The most important fact in Fig. 11 is that there is no difference between the static friction force and the kinematic one. Fig. 12 shows the relation between the coefficient of kinematic friction and the sliding velocity. The values of data measured in Test II, which were carried out after a large number of tests, are about 20% larger than them in Test I, but this should be adopted for the design value because the friction damper only works when an earthquake occurs.

RUBBER BEARING TEST: Fig. 13 shows an example of characteristics of the horizontal stiffness of rubber bearings and the fluctuations of the vertical loads. The frequency dependence of the horizontal spring constant, as shown in Fig. 14, is very low and there is little difference in the characteristics of each specimen. However, the horizontal stiffness seems to be bigger when the vertical loads are reduced. Fig. 15 shows the displacement dependence of the horizontal spring constant. The horizontal stiffness seems to be smaller in larger deflexions. Fig. 16 and Fig. 17 show a characteristic of vertical stiffness of the rubber bearing compared with the isolation device's and the frequency dependence respectively. However, the results seemed

to involve many errors in measuring the very little displacements using this set-up. So, the data, measured with more accuracy by the other way of testing, are also put in Fig. 17. Moreover, the horizontal and the vertical damping ratio of the laminated rubber bearing, calculated from the each hysterisis loop, is at least 3.2% and 11.2% respectively.

ISOLATION DEVICE TEST: Fig. 18(a) shows the characteristics of the isolation device and the rubber bearing under the same conditions. (b) shows the fluctuations of the vertical loads. It is considered that the characteristic of the isolation device is the addition of the characteristic of the laminated rubber bearing and the friction damper. Then Fig. 18(c) is obtained by the reason mentioned above. However, this hysterisis loop possesses a slight slant, therefore, (d) is obtained by the additional adjustment. Fig. 19 shows the vertical displacements of the isolation device caused by the horizontal displacement. Considering the increase of friction force by the vertical displacement, the dashed line in Fig. 18(d) is obtained and shows a good relation with the solid line. Therefore, the adjustment of the hysterisis loop in Fig. 18 is correct and this result shows that the horizontal stiffness measured in isolation device test is higher than in rubber bearing test as shown in Fig. 15. The fact mentioned above seems to consist of the following reasons; first, the vertical sliding plate as shown in Fig. 10 is loosely jointed and makes considerable slants in larger horizontal displacements and secondly, the reduction of the vertical loads on the laminated rubber bearing makes its stiffness higher as shown in Fig. 14 (the friction damper supports some portion of the vertical loads in this case). Fig. 20 shows a part of the hysterisis loop of the isolation device in excessive displacements. Last of all, Table 1 shows the good relations between the designed values and the experimented ones of the laminated rubber bearing when a vertical load of 98kN(10000kgf) is supported.

CONCLUSIONS

From the results of the experimental tests, the isolation device, manufactured by trial, is verified to satisfy the required performances when it was designed.

The authors like to express their gratitude to Mr. Suzuki, Bridgestone Tire Co., Ltd., for helping the experimental tests.

REFERENCES

1) Skinner, R. I., et al., International Journal of Earthquake Engineering and Structural Dynamics, Vol. 3, pp. 297-309 (1975).
2) Freakley, P. K. and Payne, A. R., " Theory and Practice of Engineering with Rubber ", Applied Science Publishers (1978).

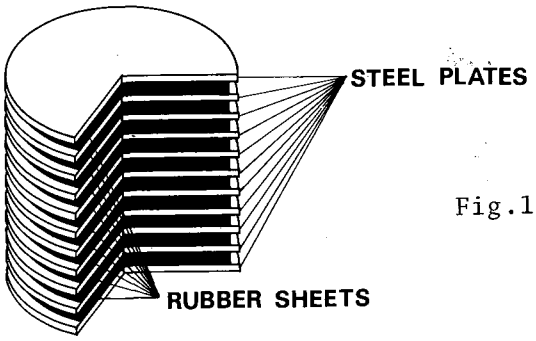

Fig.1 Schematic drawing of Rubber Bearing

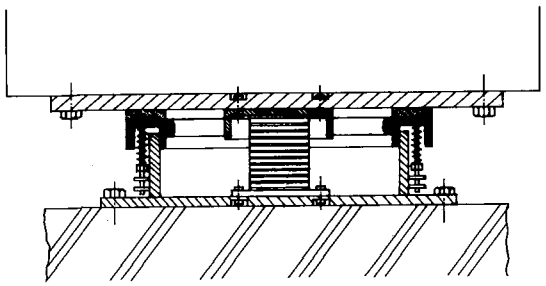

Fig.2 Schematic drawing of Isolation Device

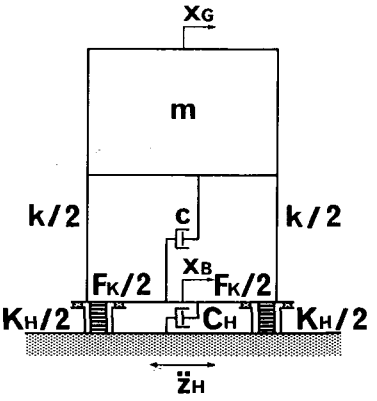

Fig.3 Analytical model of equipment with Isolation Device

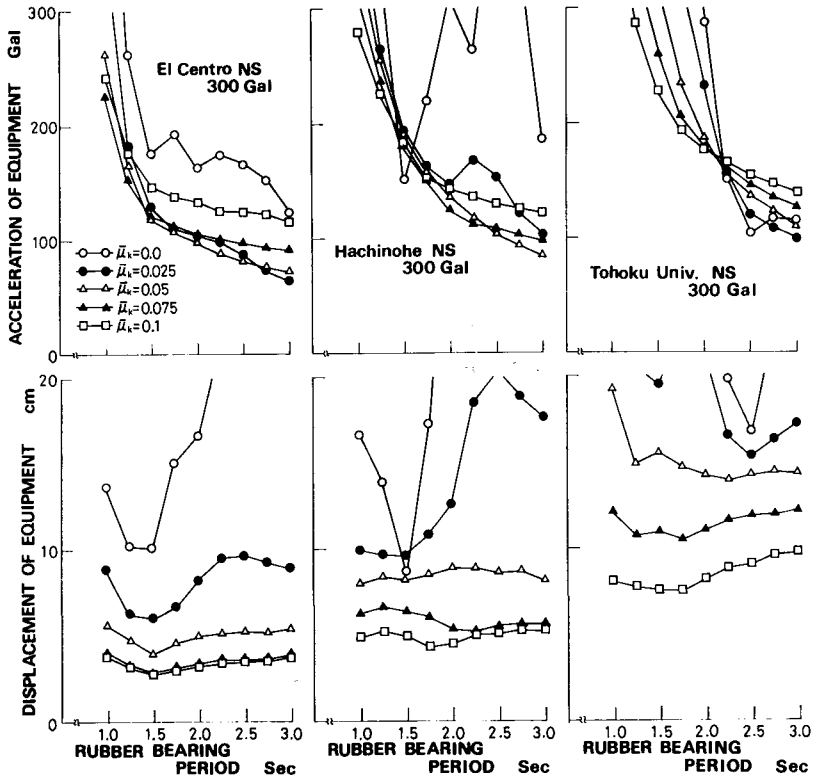

Fig.4 Effects of T_H and $\bar{\mu}_K$ on response acceleration and displacement of equipment
($\omega_0/2\pi=5$Hz , $\eta=\zeta_H=0.03$, $\bar{\mu}_S=\bar{\mu}_K$)

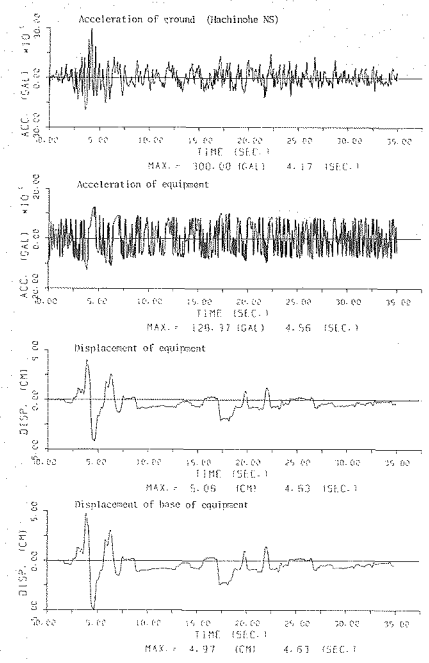

Fig.5 Time histories (Hachinohe NS 300 Gal , T_H=2.0s , $\overline{\mu}_K$= $\overline{\mu}_S$=0.08 , $\omega_0/2\pi$=5Hz $\eta=\zeta_H$=0.08)

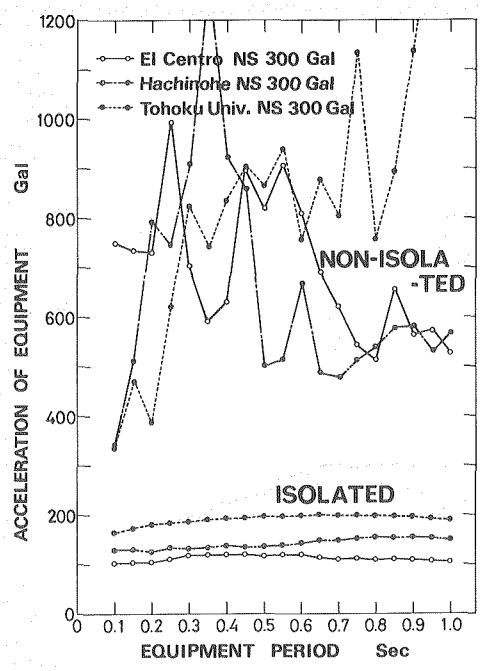

Fig.6 Maximum response acceleration of both isolated and non-isolated superstructure (T_H = 2.0s , $\eta=\zeta_H$ =0.03 $\overline{\mu}_K=\overline{\mu}_S$=0.08)

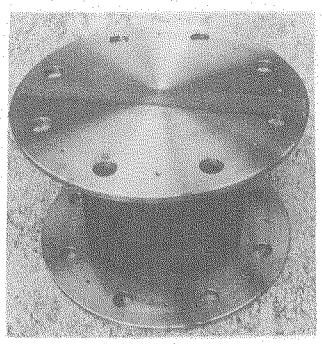

Fig.7 The Laminated Rubber Bearing

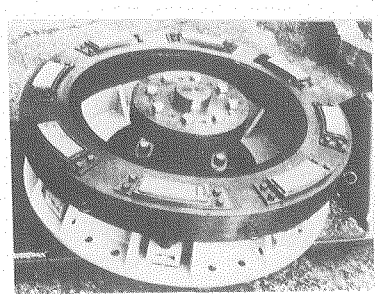

Fig.8 The Isolation Device

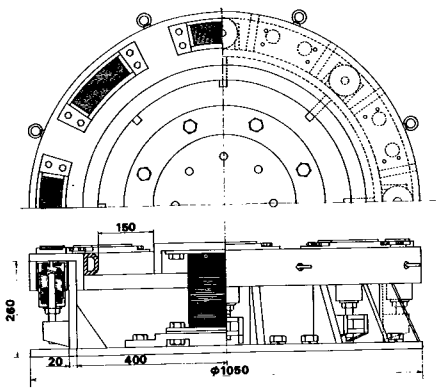

Fig.9 Dimension of the Isolation Device

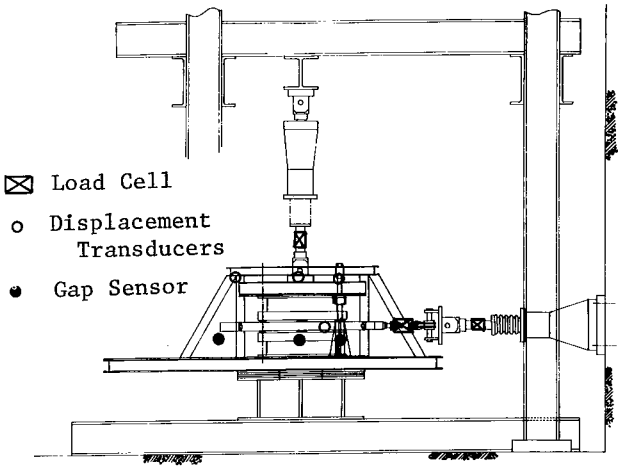

Fig.10 Schematic drawing of the experimental apparatus and installations of the transducers used in the test

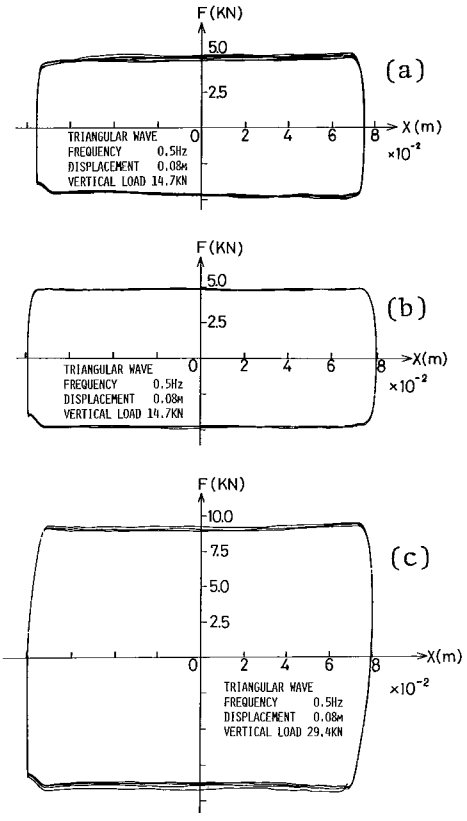

Fig.11 Force-displacement hysterisis loops of the Friction Damper

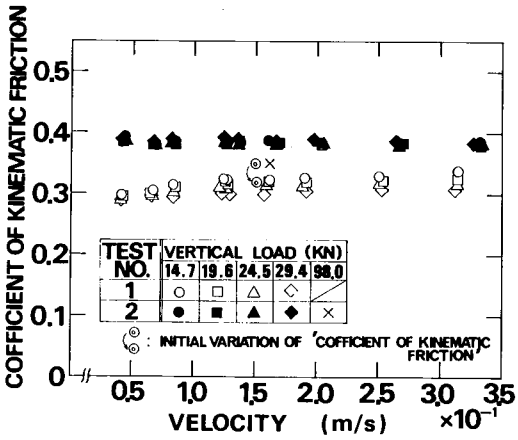

Fig.12 Relation between coefficient of kinematic friction and velocity

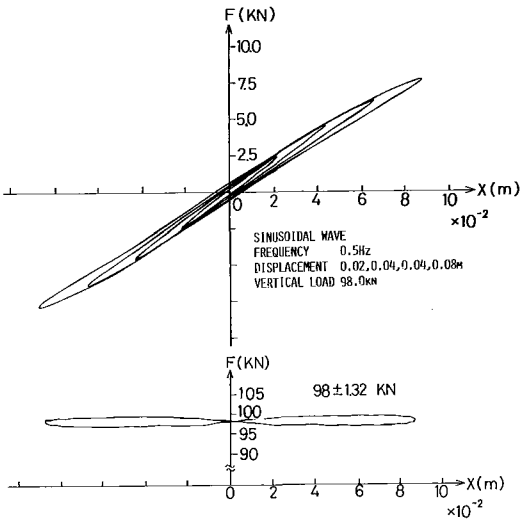

Fig.13 Horizontal stiffness of the Rubber Bearing and the vertical load

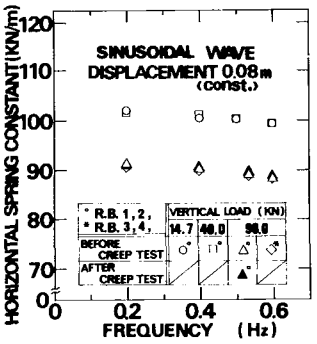

Fig.14 Horizontal spring const. vs. frequency

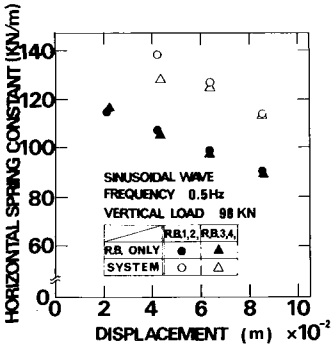

Fig.15 Horizontal spring const. vs. disp.

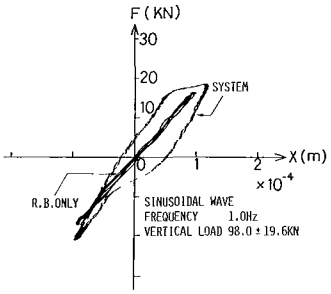

Fig.16 Vertical stiffness of the Rubber Bearing

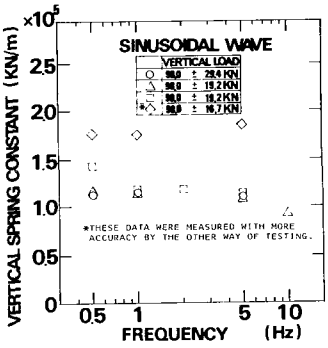

Fig.17 Vertical spring const. vs. frequency

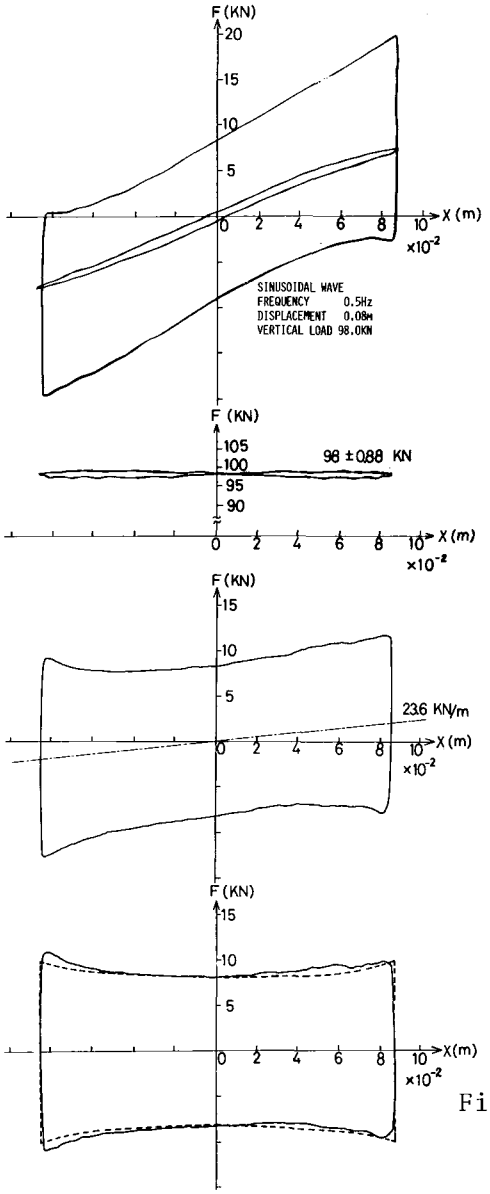

Fig.18 Force-displacement hysterisis loops of the Isolation Device

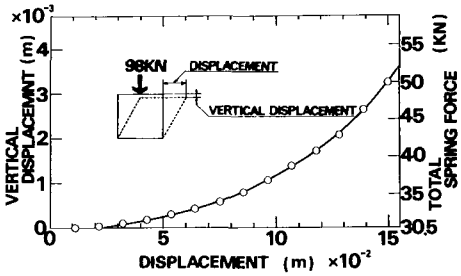

Fig.19 Relation between vertical displacement and horizontal displacement

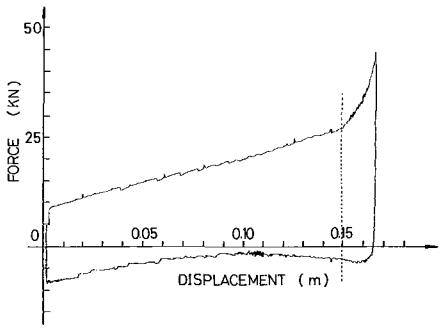

Fig.20 Force-displacement hysterisis loop of the Isolation Device

Table 1 Designed and Experimented Values of the Laminated Rubber Bearing

	Spring Constant (KN/m)		Natural frequency (Hz)	
	Horizontal	Vertical	Horizontal	Vertical
Designed	86 ∿ 113	1.4×10^5	0.47 ∿ 0.53	19.0
Exp.	88 ∿ 137	1.78×10^5	0.47 ∿ 0.59	21.3